Title

The carboxy terminal transmembrane domain of SPL7 mediates interaction with RAN1 at the endoplasmic reticulum to regulate ethylene signalling in Arabidopsis

Authors

Yang, Yanzhi

Hao, Chen

Du, Jianmei

et al.

Peer reviewed

The carboxy terminal transmembrane domain of SPL7 mediates interaction with RAN1 at the endoplasmic reticulum to regulate ethylene signalling in Arabidopsis

Yanzhi Yang[1] (iD), Chen Hao[1] (iD), Jianmei Du[2] (iD), Lei Xu[2] (iD), Zhonglong Guo[1] (iD), Dong Li[3] (iD), Huaqing Cai[3] (iD), Hongwei Guo[4] (iD) and Lei Li[1,2] (iD)

[1]State Key Laboratory of Protein and Plant Gene Research, School of Life Sciences and School of Advanced Agricultural Sciences, Peking University, Beijing 100871, China; [2]Peking-Tsinghua Center for Life Sciences, Academy for Advanced Interdisciplinary Studies, Peking University, Beijing 100871, China; [3]National Laboratory of Biomacromolecules, CAS Center for Excellence in Biomacromolecules, Institute of Biophysics, Chinese Academy of Sciences, Beijing 100101, China; [4]Department of Biology, Institute of Plant and Food Science, Southern University of Science and Technology, Shenzhen, Guangdong 518055, China

Author for correspondence:
Lei Li
Email: lei.li@pku.edu.cn

Summary

• In Arabidopsis, copper (Cu) transport to the ethylene receptor ETR1 mediated using RAN1, a Cu transporter located at the endoplasmic reticulum (ER), and Cu homeostasis mediated using SPL7, the key Cu-responsive transcription factor, are two deeply conserved vital processes. However, whether and how the two processes interact to regulate plant development remain elusive.

• We found that its C-terminal transmembrane domain (TMD) anchors SPL7 to the ER, resulting in dual compartmentalisation of the transcription factor. Immunoprecipitation coupled mass spectrometry, yeast-two-hybrid assay, luciferase complementation imaging and subcellular co-localisation analyses indicate that SPL7 interacts with RAN1 at the ER via the TMD.

• Genetic analysis revealed that the ethylene-induced triple response was significantly compromised in the *spl7* mutant, a phenotype rescuable by RAN1 overexpression but not by SPL7 without the TMD. The genetic interaction was corroborated by molecular analysis showing that SPL7 modulates RAN1 abundance in a TMD-dependent manner. Moreover, *SPL7* is feedback regulated by ethylene signalling via EIN3, which binds the *SPL7* promoter and represses its transcription.

• These results demonstrate that ER-anchored SPL7 constitutes a cellular mechanism to regulate RAN1 in ethylene signalling and lay the foundation for investigating how Cu homeostasis conditions ethylene sensitivity in the developmental context.

Introduction

Copper (Cu) is an essential transition metal in plants. Due to its excellent redox potential, Cu serves as a critical cofactor for numerous enzymes and electron carriers (Burkhead *et al.*, 2009; Robinson & Winge, 2010; Merchant *et al.*, 2020; Ishka *et al.*, 2022). Consequently, Cu is required for multiple plant growth and development processes, including, for example, the photosynthetic electron transport (Katoh, 1960; Weigel *et al.*, 2003; Zhang *et al.*, 2014), cell wall remodelling (Berthet *et al.*, 2011; Zhuang *et al.*, 2020) and seed germination (Jiang *et al.*, 2021). However, free monovalent Cu drives redox chemistry that is highly toxic to macromolecules (Burkhead *et al.*, 2009; Robinson & Winge, 2010). A strong chelating capacity is present in the cytosol of eukaryotic cells that allows for less than one free Cu ion per cell (Rae *et al.*, 1999; Finney & O'Halloran, 2003). As a result, elaborate transport systems and

partition mechanisms have evolved in eukaryotes for the precise allocation of Cu to specific target proteins (Burkhead *et al.*, 2009; Robinson & Winge, 2010; Hoppen *et al.*, 2019).

SQUAMOSA-PROMOTER BINDING PROTEIN-LIKE 7 (SPL7) in Arabidopsis and its orthologous SBP domain containing transcription factors that modulate Cu homeostasis in the green plant lineage (Kropat *et al.*, 2005; Yamasaki *et al.*, 2009; Merchant *et al.*, 2020). The SBP domain consists of two unconventional zinc fingers overlapping with a bipartite nuclear localisation signal (NLS) and therefore facilitates nuclear import of SPL7 and confers selectivity for DNA binding (Yamasaki *et al.*, 2004, 2009; Birkenbihl *et al.*, 2005; Yang *et al.*, 2008). In both Arabidopsis and the green alga *Chlamydomonas reinhardtii*, it has been shown that the SPL7 orthologues regulate the expression of genes related to Cu homeostasis, many of which possess the GTAC motif-containing Cu response elements in their

promoters (Kropat *et al.*, 2005; Yamasaki *et al.*, 2009; Sommer *et al.*, 2010; Zhang & Li, 2013; Zhang *et al.*, 2014). Structural and functional analyses suggested that Cu ions could inhibit the DNA-binding activity of the SPL7 orthologues by displacing zinc bound to the SBP domain (Kropat *et al.*, 2005; Sommer *et al.*, 2010). Based on these findings, it is proposed that SPL7 acts as a Cu sensor in the nucleus to regulate gene expression in response to changes in cellular Cu levels.

Ethylene is a small gaseous signalling molecule that exerts potent effects on plant growth, development, and response to environmental stresses (Johnson & Ecker, 1998; Merchante *et al.*, 2013; Dubois *et al.*, 2018). Perception of the ethylene signal is intrinsically connected to Cu homeostasis. The receptor proteins, exemplified by ETHYLENE RESPONSE 1 (ETR1) in Arabidopsis, are cuproproteins localised on the endoplasmic reticulum (ER) membrane that form tripartite complexes with Cu and ethylene to enable perception of the hormone (Rodriguez *et al.*, 1999; Chen *et al.*, 2002). The tripartite receptor complexes deactivate the negative regulator CONSTITUTIVE TRIPLE RESPONSE 1 (CTR1) (Kieber *et al.*, 1993; Clark *et al.*, 1998). The signal is then relayed from the ER to the nucleus by proteolytic regulation of ETHYLENE INSENSITIVE 2 (EIN2) (Alonso *et al.*, 1999; Qiao *et al.*, 2012; Wen *et al.*, 2012; Li *et al.*, 2015), where stabilisation of two paralogous transcription factors, EIN3 and EIN3-LIKE 1 (EIL1), programme the expression of the vast majority of ethylene-responsive genes (Chao *et al.*, 1997; Solano *et al.*, 1998).

Delivery of Cu to the ethylene receptors requires RESPONSIVE-TO-ANTAGONIST 1 (RAN1). Functioning in the endomembrane system, RAN1 is a P-type ATPase that transports Cu to the ER lumen (Hirayama *et al.*, 1999; Woeste & Kieber, 2000). Strong loss-of-function *ran1* alleles completely abolish ethylene-binding activity of the receptors (Woeste & Kieber, 2000; Binder *et al.*, 2010). By contrast, weak *ran1* alleles result in ethylene-like response to the ethylene antagonist *trans*-cyclo-octene, an effect that can be partially suppressed by Cu supplementation (Hirayama *et al.*, 1999). Without Cu, as manifested in the *ran1* loss-of-function mutants or the presence of Cu chelators, the receptors are permanently disabled, leading to constitutive activation of downstream signalling events (Hirayama *et al.*, 1999; Woeste & Kieber, 2000; Zhao *et al.*, 2002; Binder *et al.*, 2010; Li *et al.*, 2017). Despite this knowledge of the critical requirement of Cu in ethylene perception, how the ethylene signalling pathway interacts with the SPL7-based cellular Cu homeostasis mechanism to regulate plant response to the hormone remains largely unexplored.

In addition to the nucleus, SPL7 contains a putative C-terminal transmembrane domain (TMD) and transiently expressed SPL7 may localise to the ER (Garcia-Molina *et al.*, 2014). The current study was aimed to functionally investigate the TMD of SPL7 (SPL7^{TMD}). Cell biology experiments demonstrated that SPL7^{TMD} is necessary and sufficient for targeting SPL7 to the ER membrane, where it interacts with RAN1. Genetic analysis in Arabidopsis revealed that SPL7^{TMD} is required for regulating RAN1 abundance and ethylene sensitivity. Molecular biology studies have shown that EIN3 binds to the *SPL7* promoter and transcriptionally represses SPL7 expression in the presence of

ethylene. Together, these results indicate that ER-anchored SPL7 constitutes a cellular mechanism to regulate plant sensitivity to the ethylene signal by modulating RAN1 that transfers Cu ion to the ethylene receptors.

Materials and Methods

Plant materials and growth conditions

The wild-type plant used in this study was *Arabidopsis thaliana* ecotype Col-0. The *ein3 eil1* line has been described previously (Kieber *et al.*, 1993; Alonso *et al.*, 2003). To express full-length SPL7 and its various truncations in Arabidopsis, the respective coding sequences were cloned into the *pJim19-eGFP* binary vector under the control of the CaMV *35S* promoter. The resulting constructs were introduced into the wild-type or *spl7-1* background using standard *Agrobacterium*-mediated transformation. Transformants were selected with 50 mg l^{-1} hygromycin (Roche), allowed to propagate to the T$_3$ generation, and multiple homozygous lines identified for subsequent experiments. To express RAN1, the coding sequence was cloned into the *pJim19-eGFP* vector. The resulting *35S:RAN1-GFP* construct was introduced into the wild-type plant, selected with 50 mg l^{-1} kanamycin (Roche), and allowed to propagate to the T$_3$ generation. Identified homozygous lines were crossed with *spl7-1* to generate the *35S:RAN1-GFP spl7-1* plants.

The coding region of HY5 was cloned into the *pJIM19-mCherry* vector to generate *35S:mCherry-HY5* as a nucleus marker. The *35S:WAK2-mCherry-HDEL* (*ER-mCherry*) construct was generated using the *pJIM19-mCherry* vector to express an ER localisation marker as previously described (Nelson *et al.*, 2007). In brief, the ER marker was created by first inserting the HDEL ER retention signal at the C-terminus of mCherry using a synthetic oligonucleotide (5′-CATGACGAGCTGTAACTGCAG). Subsequently, the signal peptide of WAK2 was cloned to the N-terminus of mCherry-HDEL (Nelson *et al.*, 2007). These constructs were introduced individually into the *35S:SPL7$^{1–215}$-GFP*, *35S:SPL7$^{746–818}$-GFP*, or *35S:SPL7^{TMD}-GFP* plants via *Agrobacterium*-mediated transformation to generate the *mCherry-HY5 SPL7$^{1–215}$-GFP*, *ER-mCherry SPL7$^{746–818}$-GFP* and *ER-mCherry SPL7^{TMD}-GFP* plants, respectively. Primers used for cloning and genotyping are listed in Supporting Information Table S1.

To grow Arabidopsis seedlings, seeds were surface sterilised and plated on agar-solidified Murashige and Skoog medium containing 1% (w/v) sucrose. The plates were incubated at 4°C for 3 d in the dark and then transferred to a growth chamber with 23°C/21°C, 16 h : 8 h, light : dark settings. Adult plants were maintained in commercial soil and 16 h : 8 h, light : dark conditions, with 120 μmol m^{-2} s^{-1} light intensity provided by white fluorescence bulbs, 50% relative humidity and a temperature of 23°C/21°C. Tobacco (*Nicotiana benthamiana*) plants used for transient expression experiments were maintained in a growth chamber with 16 h : 8 h, light : dark conditions, a light intensity of *c.* 200 μmol m^{-2} s^{-1}, a relative humidity of 50% and a temperature of 25°C/21°C.

Chemical treatments

Triplin (1-(1-morpholino-1-(thiophen-2-yl) propan-2-yl)-3-(2-(trifluoromethoxy) phenyl) thiourea) (Life Chemicals) was dissolved in 1% DMSO and added to the standard Murashige & Skoog medium to a final concentration of 10 or 20 μM. Bathocuproinedisulfonic acid (BCS) or 1-amino-cyclopropane-1-carboxylic acid (ACC) (Sigma-Aldrich) was dissolved in water and added to the medium at the indicated final concentrations. Gaseous ethylene treatment of Arabidopsis seedlings was performed as previously described (Qiao *et al.*, 2012). Seedlings were grown on plates in an air-tight container kept in the dark. Ethylene was injected into the container to a final concentration of 20 ppm. Vernalised seeds plated on medium containing various combinations of the chemical treatments were allowed to grow in the dark for *c.* 4 d after germination. Hypocotyls were perpendicularly photographed using a digital camera, and the length and hook curvature were measured using IMAGEJ software. Replicates were individual seedlings.

Quantitative transcript analyses

Seedlings were homogenised with liquid nitrogen to isolate total RNA using TRIzol (Invitrogen), which was treated with DNase I (TaKaRa, Dalian, China) and reverse transcribed using the PrimeScript II 1st Strand cDNA Synthesis Kit (TaKaRa). qPCR was performed using the SYBR Green master mix on an ABI 7500 Fast Real-Time PCR System (Applied Biosystems, Shanghai, China). *ACTIN7* was used as the internal control and normalisation standard. Replicates were individual qPCR performed on the same RT reaction. All experiments were repeated at least three times and one set of representative experiment was shown (Table S2). Differential expression was called using a two-fold change cutoff. Primers used for qPCR are listed in Table S1.

Fluorescence microscopy

For transient expression in tobacco leaf epidermal cells, *Agrobacterium* GV3101 cells harbouring the *35S:SPL7-GFP*, *35S: SPL7$^{\Delta TMD}$-GFP*, *35S:SPL7$^{1-215}$-GFP*, *35S:SPL7$^{1-746}$-GFP*, *35S: SPL7$^{\Delta NLS}$-GFP*, *35S:SPL7$^{746-818}$-GFP*, or *35S:SPL7^{TMD}-GFP* construct were mixed with GV3101 cells harbouring the *35S: mCherry-HY5*, *35S:ER-mCherry*, or *35S:RAN1-mCherry* construct and co-infiltrated into the leaf epidermis with a syringe. After 3 d, the cells were observed using an LSM 800 laser scanning confocal microscope (Zeiss). Fluorescence microscopy analysis of proteins stably expressed in Arabidopsis was performed on 7-d-old seedlings. Cells in the root and the cotyledon were analysed using an LSM 800 laser scanning confocal microscope. Line-scan co-localisation was carried out using IMAGEJ software.

LUC complementation imaging

The assay was performed as described (Jing *et al.*, 2016) with minor modifications. Briefly, the coding sequences of various SPL7 forms and RAN1 were cloned into the *pCAMBIA1300-nLUC* and *pCAMBIA1300-cLUC* vector, respectively, to generate the N-terminal or C-terminal luciferase fusion constructs. The *pCAMBIA1300-nLUC* or *pCAMBIA1300-cLUC* vector alone was used as a control. *Agrobacterium* GV3101 cells harbouring the desired constructs were resuspended in the infiltration buffer to an OD$_{600}$ of 0.8. The *35S:P19-HA* (Jing *et al.*, 2016) construct and the suspension were co-infiltrated into tobacco leaf epidermis with a syringe. After 2 d, the leaves were sprayed with 20 mg ml^{-1} potassium luciferin (Gold Biotech) and incubated in the dark for 5 min. LUC activity was detected using the NightShade LB 985 system (Berthold) with an exposure time of 5 min. Replicates were individual infiltration events.

Promoter activity assays

LUC assays for promoter activity were performed as previously described (Xie *et al.*, 2017). Briefly, tobacco leaves were co-infiltrated with the *35S:GFP* or the *35S:EIN3-GFP* effector construct along with the *pSPL7:LUC* reporter construct and incubated at 25°C for 3 d. The infiltrated leaf area was imaged for luciferase luminescence. Quantification of luciferase activity was performed using INDIGO (v.2.03.0). Replicates were individual infiltration events. The REN/LUC dual luciferase assays were performed as described (Liu *et al.*, 2014) by cloning the promoter regions into the *pGreen II 0800-LUC* vector. Tobacco leaf protoplast isolation and DNA transfection were performed as described (http://molbio.mgh.harvard.edu/sheenweb/protocols_reg/protocols_reg_.php#proto_reg). Transformed protoplasts were collected, homogenised, and dual luciferase reactions carried out using the Dual-Glo Luciferase Assay System (Promega). Luciferase activity was quantified using a Multimode Reader LB 942 luminometer (Berthold, Bad Wildbad, Baden Württemberg, Germany). Replicates were individual transfection events.

Cellular fractionation

The membrane fraction of total protein was isolated from *c.* 500 mg of Arabidopsis seedlings as previously described (Zhao *et al.*, 2002). The cellular homogenate was sequentially centrifuged at 8000 *g* for 5 min and then at 100 000 *g* for 30 min. The membrane pellet was resuspended in a membrane wash buffer (10 mM Tris at pH 7.5, 150 mM NaCl, 1 mM EDTA, and 10% glycerol with protease inhibitors). The supernatant consisting of the cytosolic fraction was collected for further analysis. The nucleus fraction of total protein was isolated from 1-g seedlings as previously described (Cho *et al.*, 2006). The homogenate was filtered through a double layer of Miracloth and centrifuged for 10 min at 1000 *g* at 4°C. The pellets containing the nuclear fraction were washed with 5 ml NIB buffer (20 mM Tris–HCl at pH 7.4, 25% glycerol, 2.5 mM MgCl$_2$, 30 mM β-mercaptoethanol, 0.5% Triton X-100, 1 mM phenylmethylsulfonyl fluoride and 1× protease inhibitor cocktail) three times. The nuclear pellet was resuspended in 200 μl 2× sodium dodecyl sulphate (SDS) protein extraction buffer (80 mM Tris–HCl pH 6.8, 4% SDS, 4 mM β-mercaptoethanol, 8% glycerol and 0.02% bromophenol blue).

Protein detection

Following electrophoresis, standard immunoblotting analyses were performed. The blots were probed with either a custom rabbit anti-RAN1 polyclonal antibody, which was raised against the N-terminal 299 amino acids of RAN1, or a custom rabbit anti-SPL7 polyclonal antibody, which was raised against amino acids 418 to 752 of SPL7. Antibody for GFP (AE012; Abclonal, Wuhan, China) was used to detect GFP and YFP fusion proteins. Antibodies for H^+-ATPase (AS07 260; Agrisera, Vännäs, Sweden) and binding immunoglobulin protein (BiP) (AS09 481; Agrisera), ACTIN (CW0264; Cwbio, Taizhou, China), and H3 (H0164; Sigma-Aldrich) were used as loading standard for the membrane fraction, the cytosolic fraction and the nucleus fraction, respectively. Protein detection was performed using the ChemiDoc XRS+ imaging system (Bio-Rad). Relative protein levels were quantified using IMAGEJ software. Replicates for immunoblotting experiments were individual protein preps.

IP-MS/MS

Total protein was isolated from 10-d-old *35S:GFP* and *35S:SPL7^{746–818}-GFP* seedlings with an extraction buffer containing 25 mM Tris–HCl at pH 7.5, 150 mM NaCl, 10% glycerol, 0.5% NP40, 1 mM EDTA, 0.5 mM Na_3VO_4, 1 mM DTT, 1 mM PMSF, and 1× protease inhibitor cocktail (Roche). Following affinity purification using anti-GFP affinity beads (SA070005; Smart-Lifesciences, Changzhou, China), equal amounts of proteins from *35S:GFP* and *35S:SPL7^{746–818}-GFP* were gel separated, digested with porcine trypsin (Promega), and extracted as previously described (Yang *et al.*, 2021). The extracted samples were dried in a vacuum centrifuge concentrator and resuspended in 10 µM 0.1% formic acid. Liquid chromatography tandem mass spectrometry (LC–MS/MS) was performed on an Orbitrap Exploris 480 mass spectrometer interfaced with an Easy-nLC1200 liquid chromatography system (Thermo Fisher Scientific) as previously described (Yang *et al.*, 2021). The raw MS data were searched against the Arabidopsis Information Resource (https://www.arabidopsis.org) with no redundant entries using SEQUEST of PROTEOME DISCOVERER (v.2.2; Thermo Fisher Scientific, Shanghai, China). False discovery rate was set at 1% for each analysis. The SPL7^{TMD}-associated proteins were identified as those recovered from *35S:SPL7^{746–818}-GFP* but not from *35S:GFP* for specificity, and with a peptide spectrum match (PSM) value greater than three for reliability.

Protein co-IP

Total protein extracts from *35S:GFP* and *35S:SPL7^{746–818}-GFP* seedlings, membrane fraction of protein extracts from wild-type and *35S:RAN1-GFP* seedlings, or nucleus fraction and membrane fraction from *35S:YFP-SPL7* seedlings were incubated with anti-GFP affinity beads (SA070005; Smart-Lifesciences) at 4°C for 1 h. The beads were washed three times with a wash buffer (25 mM Tris–HCl at pH 7.5, 150 mM NaCl, 10% glycerol, 0.5% NP40, 1 mM EDTA, 1 mM DTT with protease

inhibitors). The precipitates and input extracts were then subjected to immunoblotting analysis using the indicated antibodies.

Yeast-two-hybrid assay

Full-length as well as various SPL7 truncations and full-length RAN1 were cloned in-frame with the binding domain in the *pLexA* vector and the activation domain in the *pB42AD* vector (Clontech, Beijing, China), respectively. Combinations of the *pB42AD* and *pLexA* constructs were co-transformed into the yeast strain EGY48 (Clontech). Transformants were cultured in liquid minimal SD medium (−Ura/−His/−Trp) at 30°C until an OD_{600} of 1.2–1.5 was reached. Equal amounts of cells were collected, resuspended in distilled water, and plated on SD/Gal/Raf (−Ura/−His/−Trp) induction medium containing X-gal. Liquid assays were performed according to the Yeast β-Galactosidase Assay Kit manual (Thermo Fisher Scientific).

Phylogenetic analysis

Sequences of representative SPL7 orthologues (Table S3) were aligned using MUSCLE in MEGA X with default settings (Kumar *et al.*, 2018). An unrooted neighbour-joining tree was constructed using MEGA X by applying the neighbour-joining method. The evolutionary distance was calculated as number of amino acid substitutions per site using the Poisson correction method.

ChIP-seq analysis

ChIP-seq data to determine EIN3 binding at the *SPL7* promoter were obtained and reanalysed from a previous study (Chang *et al.*, 2013), including a series of timepoints (0, 0.25, 1, 12 and 24 h) after ethylene treatment. Raw reads were aligned to the TAIR10 Arabidopsis reference genome using BOWTIE2 (Langmead & Salzberg, 2012), allowing two mismatches and no gaps. Only uniquely mapped reads were retained, aligned to the 1.5 kb promoter region of *SPL7*, and extracted to calculate mean reads per kilo base per million mapped reads (RPKM) among the three biological replicates.

Measurement of Cu content

Here, 4-d-old etiolated seedlings grown on half-strength Murashige and Skoog medium were collected and washed twice with 1 mM EDTA and then double-distilled water. For each genotype, four independent biological samples of pooled seedlings were analysed with a NexION 350X inductively coupled plasma mass spectrometer (Perkin Elmer, Shanghai, China) as described previously (Zhang *et al.*, 2014).

Results

The conserved C-terminal TMD anchors SPL7 to the ER

Consistent with their function as a transcription factor (Kropat *et al.*, 2005; Yamasaki *et al.*, 2009; Bernal *et al.*, 2012; Zhang

et al., 2014), SPL7 orthologues in land plants and green algae all possess a conserved bipartite NLS near the amino terminus (Fig. S1a,b). However, SPL7 orthologues in angiosperm also possess a 20-amino-acid hydrophobic α-helix near the carboxy terminus that is absent in green algae (Fig. S1a,b). Interestingly, the predicted likelihood of this region forming a TMD correlated with the phylogenetic relationships of the plant lineage (Fig. S1c), suggesting that a putative TMD has specifically evolved for SPL7 orthologues in angiosperm.

To investigate whether the TMD is functional, we carried out a comprehensive assessment of SPL7 subcellular localisation. We fused the GFP to seven forms of SPL7, including the full-length ($SPL7^{1–818}$-GFP), full-length with the TMD deleted ($SPL7^{\Delta TMD}$-GFP), full-length with the NLS deleted ($SPL7^{\Delta NLS}$-GFP), a truncated variant lacking the C-terminus spanning the TMD ($SPL7^{1–746}$-GFP), a truncated variant only containing the N-terminus ($SPL7^{1–215}$-GFP), and two truncated variants composed primarily of the TMD ($SPL7^{746–818}$-GFP and $SPL7^{TMD}$-GFP) (Fig. S2a). We found that $SPL7^{1–818}$-GFP transiently expressed in tobacco leaf epidermal cells exhibited dual localisation in the nucleus and the endomembrane (Fig. S2b). Comparison of the six transiently expressed truncated versions of SPL7 showed that those without the TMD were exclusively located in the nucleus, whereas those containing the TMD exhibited endomembrane localisation (Fig. S2b). Co-expression with either mCherry-tagged nucleus marker ELONGATED HYPOCOTYL 5 (HY5) (mCherry-HY5) or an engineered ER marker (ER-mCherry) confirmed the dual localisation of full-length SPL7 (Figs 1a, S3a) and the nucleus localisation of $SPL7^{\Delta TMD}$-GFP, $SPL7^{1–746}$-GFP, and $SPL7^{1–215}$-GFP (Fig. S3b–e). By contrast, presence of $SPL7^{\Delta NLS}$-GFP, $SPL7^{TMD}$-GFP and $SPL7^{746–818}$-GFP was found in ER-like tubular membrane networks that co-localised with ER-mCherry (Fig. 1b–e). These results indicated that the TMD is both necessary and sufficient for anchoring transiently expressed SPL7 to the ER membrane.

To confirm the dual localisation of SPL7 in Arabidopsis, we generated transgenic plants expressing three SPL7 variants tagged with GFP driven by the CaMV *35S* promoter, including *35S:SPL7^{TMD}-GFP*, *35S:SPL7^{746–818}-GFP*, and *35S:SPL7^{1–215}-GFP*. Whereas the fluorescence signals in *35S:SPL7^{1–215}-GFP* were restricted to the nucleus and co-localised with the nucleus marker HY5 (Fig. S4a–e), fluorescence signals in *35S:SPL7^{TMD}-GFP* and *35S:SPL7^{746–818}-GFP* highlighted an ER network-like distribution (Figs 2a, S4f). The ER location was confirmed by co-localisation analysis with the ER-mCherry marker expressed in the same transgenic plants (Fig. 2a,b). Moreover, we performed a subcellular fractionation analysis of the *35S:SPL7^{746–818}-GFP* plants. We separated cellular compartments into the nucleus, the membrane and the cytoplasm, which were confirmed by immunoblotting analysis of marker proteins representing these compartments (Fig. 2c). Immunoblotting using an anti-GFP antibody showed that $SPL7^{746–818}$-GFP is present in the membrane fraction, but not in the nucleus and cytoplasmic fractions (Fig. 2c). Together, these results demonstrated that the TMD targets SPL7 to the ER.

SPL7 interacts with RAN1 at the ER

Towards elucidating the function of $SPL7^{TMD}$, we performed immunoprecipitation followed by liquid chromatography coupled tandem mass spectrometry (IP–LC-MS/MS) analysis of proteins precipitated by a GFP antibody in the *35S:SPL7^{746–818}-GFP* and *35S:GFP* seedlings. We identified proteins specifically associated with $SPL7^{TMD}$ as those that were recovered in *35S:SPL7^{746–818}-GFP* but not in *35S:GFP*. Following this analysis, we obtained a set of 655 candidate $SPL7^{TMD}$-associated proteins (Table S4). Markedly, essentially all ER-located proteins involved in ethylene perception and signal transduction were identified, including the receptors ETR1, EIN4 (ETHYLENE INSENSITIVE 4), and ERS1 (ETHYLENE RESPONSE SENSOR 1), RAN1 that transports Cu to the receptors, and the key signal transducers CTR1 and EIN2 (Fig. 3a).

We performed four sets of experiments to validate the interaction between SPL7 and RAN1. First, we carried out yeast-two-hybrid assays using SPL7 as the bait and RAN1 as the prey (Fig. S5a). Whereas full-length and the N-terminal portion of SPL7 both appeared self-activating (Fig. S5b), truncations that removed the AHA domain abolished this self-activation (Fig. S5c). Further testing the truncated SPL7 forms revealed that only regions spanning the TMD ($SPL7^{132–786}$ and $SPL^{746–786}$) were able to interact with RAN1 in yeast (Fig. S5c,d).

Second, we used the firefly luciferase (LUC) complementation assay to test the interaction of SPL7 and RAN1 transiently co-expressed in tobacco leaf epidermal cells. We generated various constructs expressing the N-terminal half of LUC (nLUC) or the C-terminal half of LUC (cLUC) either alone or fused in-frame with other proteins. We found that the EIN3-nLUC/cLUC-SPL7, nLUC/cLUC-SPL7, and RAN1-nLUC/cLUC combinations generated LUC signals indistinguishable from the background (Fig. 3b). By contrast, the RAN1-nLUC/cLUC-SPL7 combination produced significantly greater LUC activity (Fig. 3b). Using cLUC-$SPL7^{TMD}$ instead of cLUC-SPL7 produced the same results (Fig. 3c), indicating that the TMD was sufficient for the RAN1–SPL7 interaction in the transient expression system.

Third, we generated a custom antibody for RAN1, which detected a protein consistent with the predicted size of RAN1 at 107 kD (Fig. S6a). In Arabidopsis plants expressing the *35S:RAN1-GFP* transgene, in which full-length RAN1 was fused in-frame at its C-terminus with GFP under control of the *35S* promoter, a band of an apparent size of 135 kDa, corresponding to the RAN1-GFP chimera, was detected in addition to the endogenous RAN1 (Fig. S6b), indicating that the antibody is specific for RAN1. Using this antibody, we performed co-immunoprecipitation (co-IP) to examine the interaction between SPL7 and RAN1 in Arabidopsis. We found that an anti-GFP antibody was able to precipitate RAN1 from total protein in the *35S:SPL7^{746–818}-GFP* but not from the *35S:GFP* seedlings (Fig. 3d). Furthermore, the RAN1–SPL7 interaction in Arabidopsis was also confirmed using the *35S:RAN1-GFP* and the *35S:YFP-SPL7* (full-length SPL7 fused to yellow fluorescent protein) transgenic lines by co-IP analysis (Fig. S7a,b). Taken
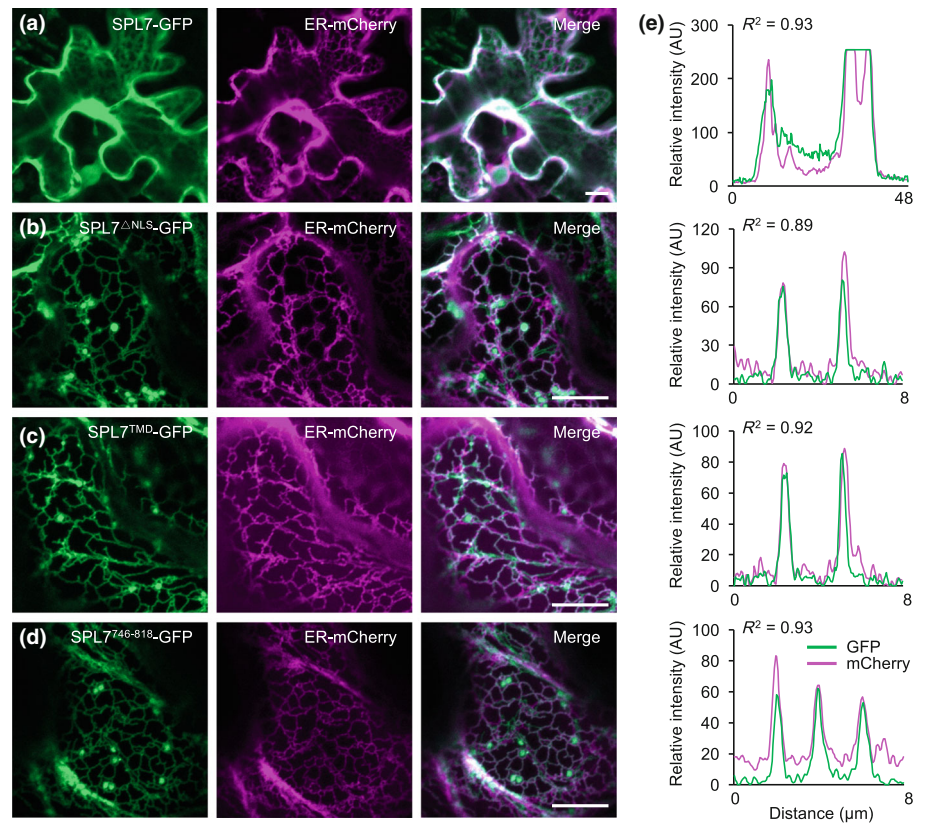
Fig. 1 Transiently expressed transmembrane domain (TMD) of SPL7 is sufficient for endoplasmic reticulum (ER) localisation. (a–d) Subcellular localisation of SPL7-GFP (a), SPL7$^{\Delta NLS}$-GFP (b), SPL7^{TMD}-GFP (c), and SPL7$^{746–818}$-GFP (d). The fluorescent proteins together with ER-mCherry, a mCherry-tagged ER marker, in tobacco epidermal cells and subjected to fluorescence microscopy examination. Bar, 10 μm. (e) Line-scan analysis of the co-localisation of SPL7-GFP, SPL7$^{\Delta NLS}$-GFP, SPL7^{TMD}-GFP and SPL7$^{746–818}$-GFP with ER-mCherry, which are shown from top to bottom. AU, arbitrary unit; R, Pearson correlation coefficient.

together, these results indicated that the TMD-mediated SPL7 interaction with RAN1 in Arabidopsis.

Finally, we pinpointed whether the RAN1-SPL7 interaction takes place at the ER. Consistent with previous reports (Hirayama *et al.*, 1999; Li *et al.*, 2017), we found that RAN1-GFP transiently expressed in tobacco cells predominantly co-localised with the ER-mCherry marker (Fig. S8). We co-expressed SPL7-GFP, SPL7$^{\Delta TMD}$-GFP, or SPL7$^{\Delta NLS}$-GFP with RAN1-mCherry in tobacco leaf epidermis for quantitatively analysing co-localisation. Compared with full-length SPL7 that exhibited nucleus–ER dual localisation, SPL7$^{\Delta TMD}$-GFP, but not SPL7$^{\Delta NLS}$-GFP, abolished co-localisation with RAN1 (Fig. 4a). This conclusion was corroborated by line-scan analysis of RAN1 co-localisation with the three SPL7 variants, which showed that the correlation coefficient between SPL7$^{\Delta TMD}$-GFP and RAN1-mCherry was drastically lower than that exhibited by SPL7-GFP and SPL7$^{\Delta NLS}$-GFP (Fig. 4b). Collectively, these results confirmed the ER localisation of the SPL7^{TMD}-mediated SPL7–RAN1 interaction.

SPL7^{TMD} is required for ethylene-induced triple response

Given the critical role of Cu in ethylene signal transduction (Hirayama *et al.*, 1999; Rodriguez *et al.*, 1999; Woeste & Kieber, 2000), we investigated whether SPL7^{TMD} is required for ethylene signalling. The so-called 'triple response' is commonly used as an ethylene-specific response, which refers to exaggerated apical hooks and shortened hypocotyls and roots of etiolated seedlings exposed to ethylene (Binder, 2020). We used the *spl7-1* mutant

containing a T-DNA insertion after the SBP domain (Fig. S9a) that had been characterised as a loss-of-function mutant (Yamasaki *et al.*, 2009; Zhang *et al.*, 2014). Treating etiolated *spl7-1* seedlings with various concentration of the ethylene precursor ACC revealed a significantly alleviated triple response, manifesting as more elongated hypocotyls and less exaggerated apical hooks compared with the wild-type seedlings (Fig. 5a–c). This result indicated that *SPL7* is necessary for proper ethylene response.

To determine whether the TMD was involved in regulating ethylene response, we expressed full-length SPL7 and SPL7 without the TMD in the *spl7-1* background to generate the *35S:SPL7-GFP spl7-1* and *35S:SPL7$^{1–746}$-GFP spl7-1* plants, respectively. Characterisation of multiple independent transgenic lines showed that the *35S:SPL7-GFP* or the *35S:SPL7$^{1–746}$-GFP* transgene was properly expressed in *spl7-1* (Fig. S9b). We found that expression levels of representative SPL7-regulated genes, including *MIR398C*, *MIR408*, and *COPT2* (*COPPER TRANSPORTER 2*) (Yamasaki *et al.*, 2009; Zhang *et al.*, 2014) were restored in *35S:SPL7-GFP spl7-1* and *35S:SPL7$^{1–746}$-GFP spl7-1* plants (Fig. S9c). Moreover, growth defects of the *spl7-1* seedlings, including smaller cotyledons, shorter roots and reduced fresh weight, were rescued to comparable levels as the wild-type in *35S:SPL7-GFP spl7-1* and *35S:SPL7$^{1–746}$-GFP spl7-1* (Fig. S10). Therefore, the C-terminal TMD is not required for the SPL7 function as a Cu-responsive transcription factor under the examined conditions.

We found that the reduced sensitivity of *spl7-1* seedlings to ACC was fully rescued in *35S:SPL7-GFP spl7-1* (Fig. 5a–c). However, compared with the wild-type and *35S:SPL7-GFP spl7-*
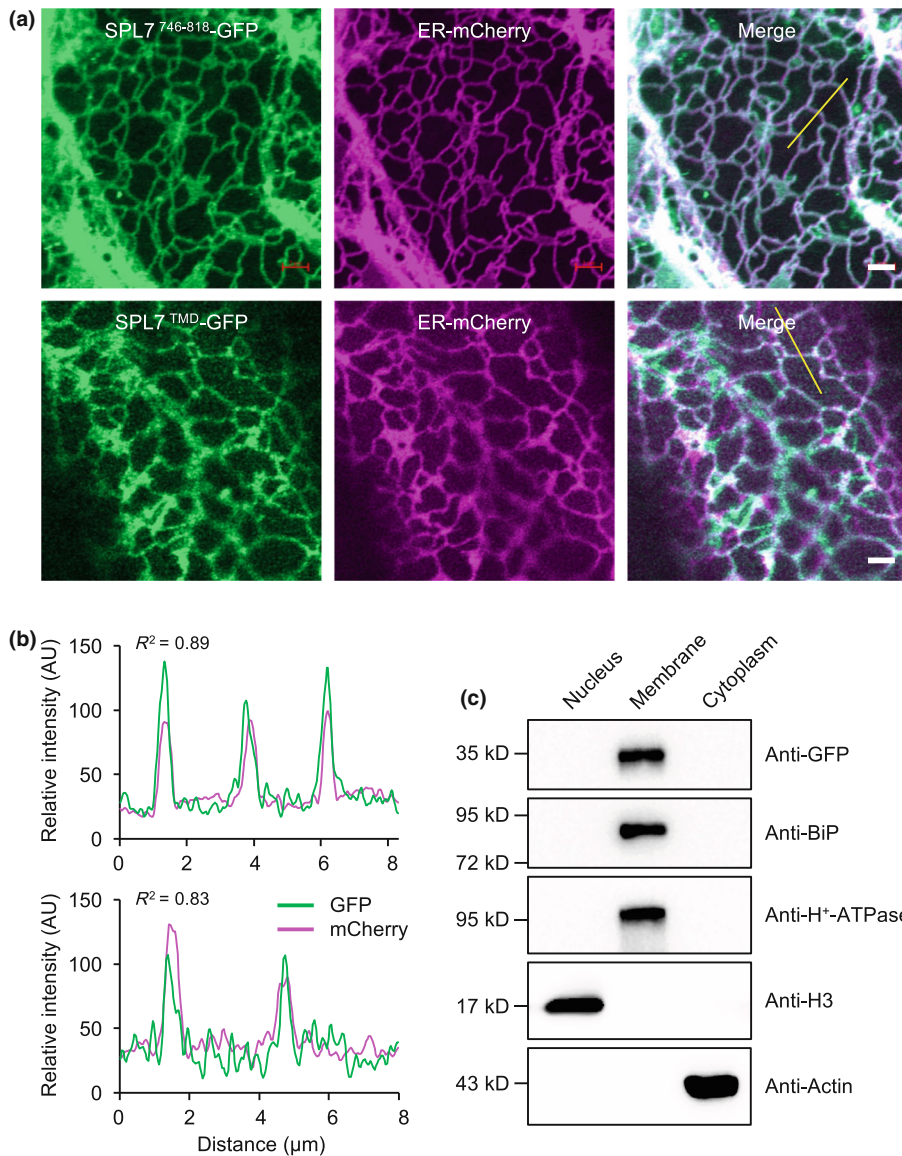
Fig. 2 The transmembrane domain (TMD) targets SPL7 to the endoplasmic reticulum (ER) in Arabidopsis. (a) Subcellular localisation of SPL7$^{746-818}$-GFP and SPL7^{TMD}-GFP. Cotyledons of 7-d-old Arabidopsis seedlings expressing *35S:SPL7$^{746-818}$-GFP* or *35S:SPL7^{TMD}-GFP* together with a mCherry-tagged ER marker were subjected to fluorescence microscopy. Bar, 2 μm. (b) Co-localisation of SPL7$^{746-818}$-GFP (upper panel) or SPL7^{TMD}-GFP (lower panel) with the ER-mCherry. Line-scan analysis was performed across the regions indicated by the yellow lines in (a). AU, arbitrary unit; *R*, Pearson correlation coefficient. (c) Cellular fractionation analysis of SPL7$^{746-818}$-GFP localisation. Nuclear, membrane, and cytosolic fractions were prepared from 10-d-old *35S:SPL7$^{746-818}$-GFP* seedlings and subjected to western blotting with the indicated antibodies. BiP (LUMINAL BINDING PROTEIN), H$^+$-ATPase, histone H3 and actin were used as markers for the ER membrane, the plasma membrane, the nucleus and the cytoplasm, respectively. Size markers are indicated on the left.

1 seedlings, *35S:SPL7$^{1-746}$-GFP spl7-1* seedlings maintained subpar triple response as the *spl7-1* mutant, based on quantification of the relative hypocotyl length and the apical curvature in response to ACC (Fig. 5a–c). To further corroborate this observation, we treated the four genotypes with gaseous ethylene. We found that 20 ppm ethylene caused a similar triple response in the etiolated wild-type and *35S:SPL7-GFP spl7-1* seedlings (Fig. S11a). However, the relative hypocotyl lengths of the *spl7-1* and *35S:SPL7$^{1-746}$-GFP spl7-1* seedlings were significantly longer after exposure to ethylene (Fig. S11b). Based on these results, we concluded that the C-terminal TMD of SPL7 was essential for proper ethylene response in Arabidopsis.
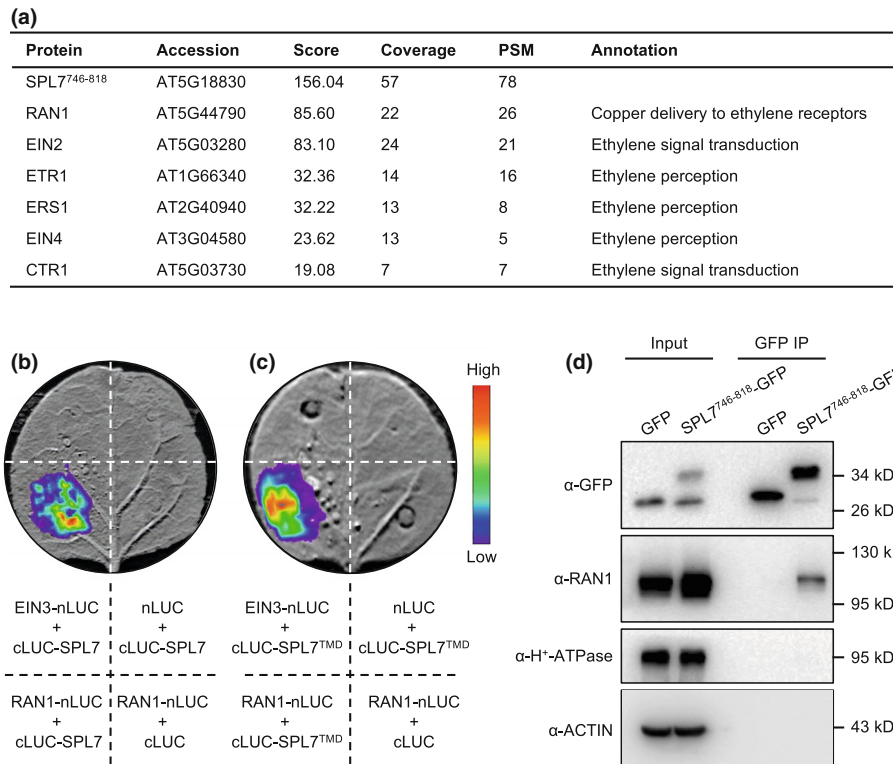
The *spl7-1* mutant is hypersensitive to Triplin-induced triple response

Because SPL7 is key to Cu homeostasis under Cu deficiency (Yamasaki *et al.*, 2009; Bernal *et al.*, 2012; Zhang *et al.*, 2014), we tested whether it was required for the ethylene response under Cu starvation. Previously it was reported that the Cu chelator Triplin causes a dose-dependent triple response in etiolated Arabidopsis seedlings (Li *et al.*, 2017). To confirm this effect, we treated wild-type seedlings with two different Triplin concentrations (10 and 20 μM) and found that the degree of hypocotyl shortening increased in response to increasing Triplin levels (Fig. S12). Moreover, Triplin treatments did not alter the morphology of the *etr1-1* and *ctr1-1* seedlings, mutants that disrupt ethylene signalling (Fig. S12). These observations indicated that the Triplin-induced triple response depended on the integrity of the ethylene signalling.

Consistent with its function in transporting Cu to the ethylene receptors, previous studies have shown that *ran1* mutants are hypersensitive to Triplin (Li *et al.*, 2017). We used seedlings harbouring the *ran1-2* allele (Fig. S6a), which contained a G173E substitution that reduces the metal-binding capacity of RAN1 (Hirayama *et al.*, 1999), to confirm the reported phenotype of the *ran1* mutants. Compared with the wild-type, Triplin caused the *ran1-2* seedlings to display a significantly more shortened

(a)

Protein	Accession	Score	Coverage	PSM	Annotation
SPL7$^{746-818}$	AT5G18830	156.04	57	78	
RAN1	AT5G44790	85.60	22	26	Copper delivery to ethylene receptors
EIN2	AT5G03280	83.10	24	21	Ethylene signal transduction
ETR1	AT1G66340	32.36	14	16	Ethylene perception
ERS1	AT2G40940	32.22	13	8	Ethylene perception
EIN4	AT3G04580	23.62	13	5	Ethylene perception
CTR1	AT5G03730	19.08	7	7	Ethylene signal transduction

Fig. 3 SPL7 interacts with RAN1 via its transmembrane domain (TMD). (a) Ethylene signalling-related proteins identified from an immunoprecipitation-mass spectrometry (IP-MS) analysis of *35S:SPL7$^{746-818}$-GFP* seedlings using a green fluorescent protein (GFP) antibody coupled to agarose beads. Score, score calculated by the Sequest HT search engine for matching the peptides to each spectrum. Coverage, the percentage coverage of the identified peptide sequence relative to the annotated protein sequence. PSM, peptide spectrum match estimating relative protein content. (b, c) Luciferase (LUC) complementation imaging assay for validating the interaction of full-length SPL7 (b) and SPL7^{TMD} (c) with RAN1. RAN1 and SPL7/SPL7^{TMD} were fused with the N- and C-terminal portions of LUC, respectively, to generate the *RAN1-nLUC* and *cLUC-SPL7/SPL7^{TMD}* constructs. The constructs were combined with either *cLUC*, *nLUC* or *EIN3-nLUC* as indicated, co-expressed in tobacco leaf epidermal cells, and imaged in the presence of luciferin. Colours indicate relative luminescence intensity. (d) Co-immunoprecipitation analysis of the SPL7–RAN1 interaction in Arabidopsis. Total proteins extracted from the *35S:GFP* and *35S:SPL7$^{746-818}$-GFP* seedlings were incubated with agarose beads coupled to an anti-GFP antibody. Input and precipitated proteins were analysed using the indicated antibodies. Size markers are indicated on the right.

hypocotyl and more exaggerated apical hook (Fig. 6a,b). We found that the Triplin-induced response was also significantly enhanced in the *spl7-1* mutant, based on quantification of the relative hypocotyl length and hook curvature (Fig. 6a,b). These effects on *spl7-1* were confirmed using another Cu chelator BCS (Fig. S13). Moreover, quantification of endogenous Cu contents revealed no significant differences between *spl7-1* and the wild-type either in the absence or the presence of Triplin (Fig. S14a, b). These results indicated that SPL7 is required for the triple response induced by Cu deficiency.

SPL7 modulates RAN1 abundance

Immunoblotting analysis revealed that the RAN1 level increased to *c.* four-fold in the *spl7-1* mutant in comparison with that of the wild-type (Fig. 7a). Consistent with their effects in restoring ethylene sensitivity of the *spl7-1* mutant, elevated RAN1 protein levels were observed in *35S:SPL7$^{1-746}$-GFP spl7-1* but not in *35S:SPL7-GFP spl7-1* compared with the wild-type (Fig. 7a). Using reverse transcription-coupled quantitative PCR (RT-qPCR), we found that the *RAN1* transcript level did not vary significantly among these genotypes (Fig. S15a). Based on these

observations, we concluded that SPL7 modulates RAN1 protein abundance in a TMD-dependent manner and that its absence elicits overcompensation of RAN1 accumulation.

To explore the mechanism by which SPL7 regulates RAN1, we performed the following sets of experiments. First, we carried out pharmacological analysis using Triplin. While RT-qPCR analysis revealed no significant changes in *RAN1* transcript abundance following Triplin treatment (Fig. S15b), immunoblotting showed that RAN1 levels increased to four-fold compared with that in the mock-treated seedlings (Fig. 7b). Moreover, we observed that RAN1 protein abundance in *ran1-2* seedlings increased to over three-fold compared with the wild-type (Fig. 7c), in the absence of a significant increase in the transcript level (Fig. S15c). These results indicate that Cu deficiency or reduced Cu delivery activity of RAN1 results in overcompensation of RAN1 accumulation as in *spl7-1* and *35S:SPL7$^{1-746}$-GFP spl7-1*. Next, we introduced the *35S:RAN1-GFP* transgene into the *spl7-1* background. In the *35S:RAN1-GFP spl7-1* seedlings, we observed that the overall level of RAN1 was elevated to *c.* 20-fold that in the wild-type and five-fold that in *spl7-1* (Figs 7d, S6b). Under these circumstances, we found that the level of endogenous RAN1 in *spl7-1* was brought down to a level
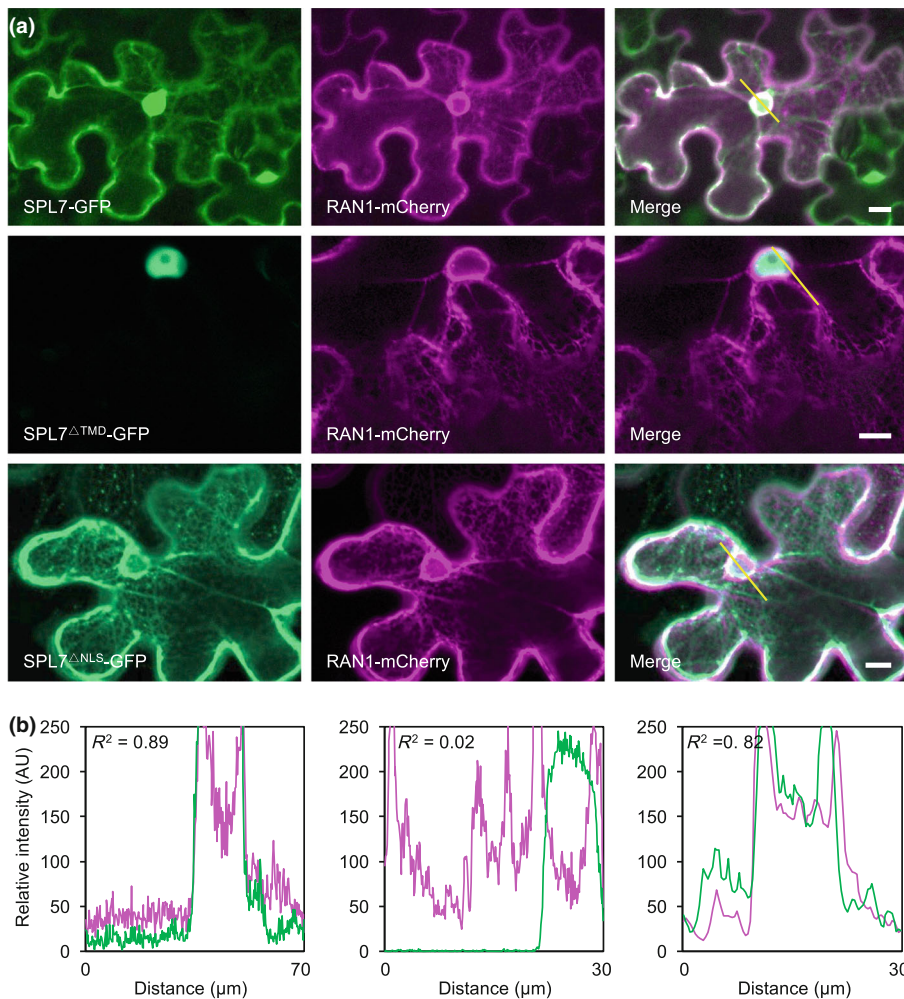
Fig. 4 The transmembrane domain (TMD) of SPL7 mediates co-localisation with RAN1. (a) Subcellular localisation of SPL7 variants. SPL7-GFP (top), SPL7$^{\Delta TMD}$-GFP (middle), or SPL7$^{\Delta NLS}$-GFP (bottom) were expressed together with RAN1-mCherry in tobacco epidermal cells and subjected to fluorescence microscopy analysis. Bar, 10 µm. (b) Line-scan analysis of co-localisation of different SPL7-GFP variants with RAN1-mCherry. Fluorescence intensities for the indicated channels were scanned in regions represented by the yellow lines in the merged images in (a). Average intensities from the two channels were separately calculated and plotted. AU, arbitrary unit; R, Pearson correlation coefficient.

comparable with that of the wild-type in *35S:RAN1-GFP spl7-1* (Fig. 7d). This finding indicated that direct elevation of RAN1 level could alleviate the compensatory effect caused by the absence of a functional SPL7. Furthermore, we compared the *spl7-1* and *35S:RAN1-GFP spl7-1* seedlings for sensitivity to ACC. Following ACC treatments, we found that both the relative hypocotyl length and the angle of the apical hook of the *35S: RAN1-GFP spl7-1* seedlings were brought to levels comparable with the wild-type but significantly different from *spl7-1* (Fig. 7e, f). Taken together, these results indicated that, through the TMD-mediated interaction with RAN1, SPL7 facilitates RAN1-based Cu delivery to the ethylene receptors for a proper response to the ethylene signal. In the absence of SPL7^{TMD}, the RAN1 level is compensatively elevated but not sufficiently enough to fully restore ethylene sensitivity.

Feedback repression of *SPL7* by ethylene signalling

Our final aim was to investigate the relationship between *SPL7* expression and ethylene signalling. This investigation was facilitated by the availability of genome-wide EIN3 binding profiles over a time course of ethylene treatment (Chang *et al.*, 2013). In the 1.5 kb upstream regulatory region starting from the

transcription start site (TSS) of the *SPL7* gene, no EIN3 binding was found before ethylene treatment (Fig. S16a). However, immediately following ethylene treatment, EIN3 binding at the *SPL7* promoter began to increase and plateaued at 1 h after ethylene treatment (Fig. S16a,b). Ethylene-induced EIN3 binding to the *SPL7* promoter declined by 4 h after treatment and returned to baseline levels by 24 h (Fig. S16a,b). These results indicated that EIN3 specifically binds to the *SPL7* promoter in response to ethylene signalling.

To validate and assess the net effect of EIN3 binding to the *SPL7* promoter, we generated a *pSPL7:LUC* construct in which the native *SPL7* promoter was used to drive the expression of the LUC reporter. We observed that LUC activity from *pSPL7:LUC* was significantly weakened when *EIN3* was used to co-infiltrate tobacco leaf epidermis (Fig. S16c), indicating that EIN3 negatively affected *SPL7* promoter activity. This conclusion was further validated by comparing the effects of EIN3 on the *SPL7* and *ERF1* (*ETHYLENE RESPONSE FACTOR 1*) promoters, using the dual LUC and *Renilla* luciferase (REN) system (Liu *et al.*, 2014). Consistent with previous reports (Solano *et al.*, 1998; Chang *et al.*, 2013), we found that EIN3 increased the promoter activity of *ERF1*, a hallmark EIN3-activated gene, transiently expressed in tobacco protoplasts (Fig. S16d). However, LUC

Fig. 5 The transmembrane domain (TMD) of SPL7 is required for proper response to 1-amino-cyclopropane-1-carboxylic acid (ACC). (a) Morphology of wild-type, *spl7-1*, *35S:SPL7¹⁻⁷⁴⁶-GFP spl7-1*, and *35S:SPL7-GFP spl7-1* etiolated seedlings treated with different concentrations of ACC. Bar, 5 mm. (b) Enlarged view of individual seedlings showing the apical hook. Bar, 1 mm. (c) Quantification of relative hypocotyl length and angle of the apical hook for the indicated genotypes following ACC treatments. Relative hypocotyl length was determined by normalisation against the untreated seedlings of the same genotype. Data represent the mean ± SD from 15 individual seedlings. Different letters denote genotypes with significant differences (one-way ANOVA, *P* < 0.001). Experiments were repeated four times with similar results.
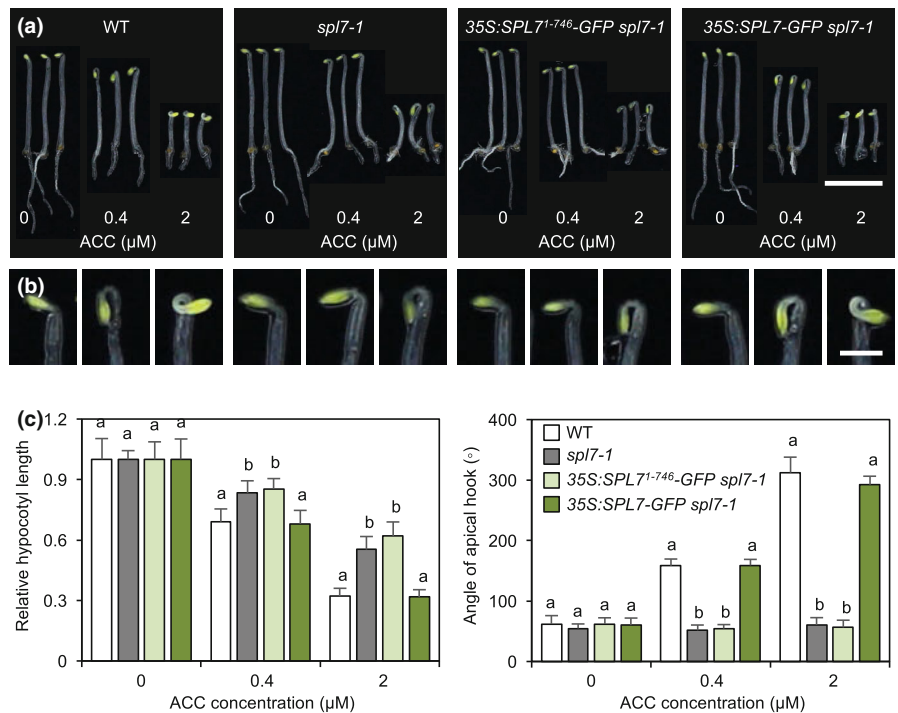
activity driven by the *SPL7* promoter was significantly weakened when *EIN3* was co-expressed (Fig. S16d), therefore confirming that EIN3 specifically represses the *SPL7* promoter.

To examine how *SPL7* responds to ethylene signalling, we stably expressed *pSPL7:LUC* in Arabidopsis. We found that ACC treatment resulted in significantly reduced LUC activity in etiolated *pSPL7:LUC* seedlings (Fig. S16e,f). Using RT-qPCR analysis, we found that the *SPL7* transcript level decreased upon ACC treatment in a concentration-dependent manner in the wild-type but not in the *ein3 eil1* double mutant that blocks transcriptional response to ethylene (Chao *et al.*, 1997) (Fig. S16g). Taken together, these results indicated that, as a positive regulator of ethylene response, *SPL7* is feedback repressed by ethylene signalling via EIN3.

Discussion

In Arabidopsis, seemingly conflicting with its function as a key transcriptional regulator of Cu homeostasis in the nucleus (Yamasaki *et al.*, 2009; Bernal *et al.*, 2012; Zhang *et al.*, 2014; Yan *et al.*, 2017), SPL7 contains a putative C-terminal TMD (Garcia-Molina *et al.*, 2014) and is predicted to pass the membrane just once with the large N-terminus outside and the short C-terminus inside the ER lumen (Fig. 8). We characterised SPL7^TMD and determined its function using four sets of experimental approaches. First, imaging and subcellular fractionation analyses of plants expressing various SPL7 truncation forms demonstrated that SPL7^TMD anchors SPL7 to the ER membrane (Figs 1, 2, S2). Second, biochemical experiments including IP-MS/MS, LUC complementation imaging, yeast-two-hybrid assay, and co-IP revealed that SPL7^TMD interacts with ER-located RAN1 (Figs 3, 4, S5, S7). This finding juxtaposed ER-

localised SPL7 to the ethylene perception machinery that consists of clusters of receptor homodimers associated with CTR1 and EIN2 in high-molecular-mass complexes at the ER (Binder, 2020). Third, genetic analysis confirmed that SPL7^TMD participates in regulating ethylene and the Cu chelation-induced triple response (Figs 5, 6, S11). Finally, biochemical analysis revealed hyperaccumulation of RAN1 under Cu deficiency, in *ran1-2*, *spl7-1*, and *35S:SPL7¹⁻⁷⁴⁶-GFP spl7-1*, but not in *35S:SPL7-GFP spl7-1* and *35S:RAN1-GFP spl7-1* (Fig. 7). These findings indicated that SPL^TMD regulates RAN1 activity and/or accumulation.

Summarising findings from the current study and previous knowledge, we proposed a working model on the role of the ER-localised SPL7 in regulating ethylene signalling (Fig. 8). In this model, the Cu-responsive transcription factor forms a module with RAN1 via its C-terminal TMD. Because only Cu-bound receptors are capable of perceiving ethylene and RAN1 is necessary for the biogenesis of the Cu-bound receptors (Rodriguez *et al.*, 1999), the physiological results (Figs 5, 6, S11) collectively demonstrated that ER-located SPL7 modulates RAN1-based Cu delivery to the ethylene receptors across the ER membrane (Fig. 8). The exact biochemical mechanism by which SPL7 regulates RAN1 function is yet to be elucidated, but it could be envisioned that SPL7 does so either directly by facilitating Cu transfer to RAN1 or indirectly by modulating RAN1 abundance (Fig. 7). As *SPL7* is transcriptionally suppressed by ethylene signalling (Fig. S16), the SPL7-RAN1 module therefore has the capacity to fine-tune ethylene sensitivity of the plant (Fig. 8).

Cu transfer between protein partners along the cellular routes is driven by gradients of increasing Cu-binding affinities (Banci *et al.*, 2010). Previous studies have shown that RAN1 acquires
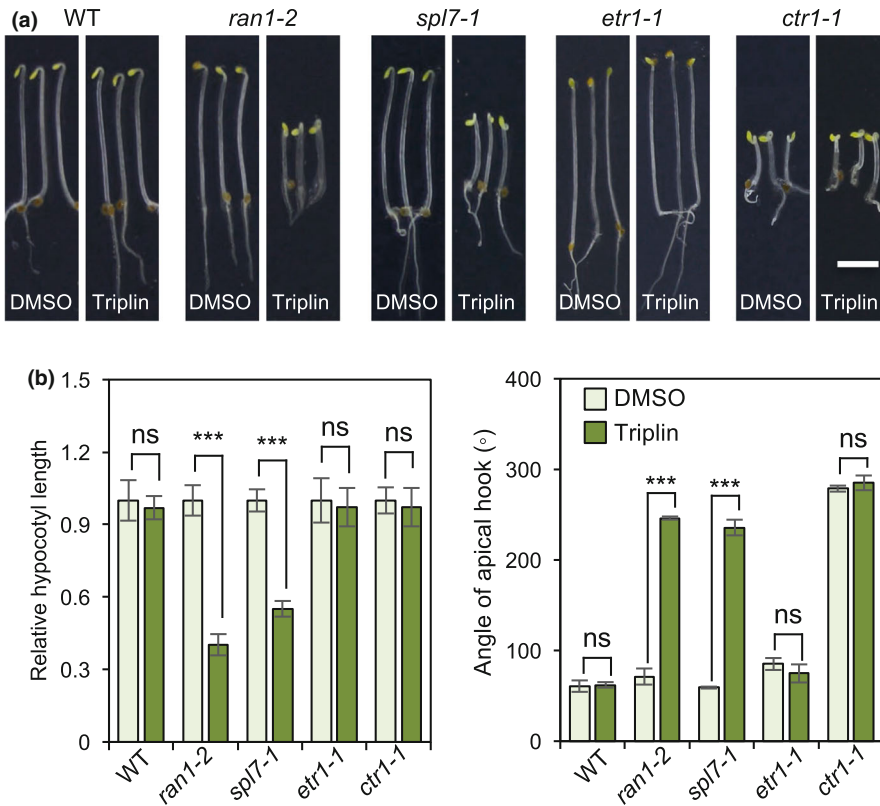
Fig. 6 The *spl7-1* mutant is hypersensitive to Cu chelation. (a) Photographs of representative etiolated seedlings of the indicated genotypes grown on medium containing 1% dimethylsulphoxide (DMSO) or 10 µM Triplin dissolved in DMSO. Bar, 2 mm. (b) Quantification of the relative hypocotyl length (left) and the angle of apical hook (right) of the etiolated seedlings. Relative hypocotyl length was determined by normalisation against the untreated seedlings of the same genotype. Data represent mean ± SD from 25 individual seedlings. ns, not significant; ***, $P < 0.001$ by Student's *t*-test. Experiments were repeated four times with similar results.

Cu from the cytosolic ATX1 chaperone family before passing the cofactor to the ethylene receptors (Li *et al.*, 2017; Hoppen *et al.*, 2019) (Fig. 8). RAN1 and ATX1 orthologues exhibited Cu-binding affinities that were approximately four orders of magnitude higher than that exhibited by SPL7 orthologues (Yatsunyk & Rosenzweig, 2007; Sommer *et al.*, 2010). Therefore, it is unlikely that Cu is drawn from ATX1 to SPL7 and then passed to RAN1. Given the recently demonstrated cupric reductase activity of histone H3 (Attar *et al.*, 2020), we speculated that the nucleus is a source for monovalent Cu and the nucleus–ER partitioning of SPL7 may serve as an alternative route for delivering Cu to RAN1 (Fig. 8). Further biochemical studies are necessary to resolve the molecular structures and dynamics of the Cu transport routes to RAN1 to substantiate the biological importance of the SPL7–RAN1 interaction.

Ethylene perception and the resulting transcriptional programming are compartmentalised to the ER and the nucleus, respectively (Chao *et al.*, 1997; Solano *et al.*, 1998; Chang & Shockey, 1999; Chen *et al.*, 2002). Fluorescence microscopy showed that GFP tagged to the C-terminus of SPL7 was observed in the nucleus (Figs 4a,b, S2b, S3a), indicating that at least a portion of the nucleus-localised SPL7 may still had an intact C-terminus and therefore the TMD. Previously it was reported that the transcriptional regulation activity of SPL7 requires farnesylation of heat shock protein 40 (Barghetti *et al.*, 2017). Therefore, it is possible that similar post-translational modification mechanisms may regulate partitioning of SPL7 between the nucleus and the ER. Alternatively, SPL7 might be subjected to proteolysis at the C-terminus that removes the TMD to allow differential subcellular localisation

of the various truncation forms. This later scenario is parallel to the regulation of EIN2, the central signal transducer that undergoes proteolytic activation and relays the ethylene signal from the ER to the nucleus (Alonso *et al.*, 1999; Qiao *et al.*, 2012; Wen *et al.*, 2012). It would be interesting to fully identify and compare the EIN2 and SPL7 proteolysis systems in future investigations to provide more insights into the interplay between Cu homeostasis and ethylene signalling. Moreover, feedback regulation of *SPL7* expression by ethylene signalling in an EIN3-dependent manner (Fig. S16) adds SPL7 to the many regulatory loops that facilitate the communication between the ER and the nucleus for properly relaying and tuning ethylene signal transduction (Merchante *et al.*, 2013). Through these interconnected regulatory feedback loops, it is anticipated that sophisticated calculations could be performed to achieve optimal cellular sensitivity to the hormone.

It was first realised half a century ago that ethylene must bind to a metal-containing receptor to enact its biological effects (Burg & Burg, 1967). Indeed, cloning of the ethylene receptor genes revealed the receptors to be cuproteins (Rodriguez *et al.*, 1999; Hirayama & Alonso, 2000). Subsequently, RAN1 was identified as the ER-located Cu transporter for the ethylene receptors (Hirayama *et al.*, 1999; Woeste & Kieber, 2000). Despite this apparent biochemical foundation for a Cu–ethylene crosstalk, the underpinning cellular mechanisms remain largely unexplored. Our findings that SPL7 modulates RAN1 abundance and participates in feedback regulation of ethylene response filled a gap in the understanding of the Cu–ethylene crosstalk. As SPL7 orthologues act as Cu sensors for regulating gene expression in response to changes in cellular Cu levels
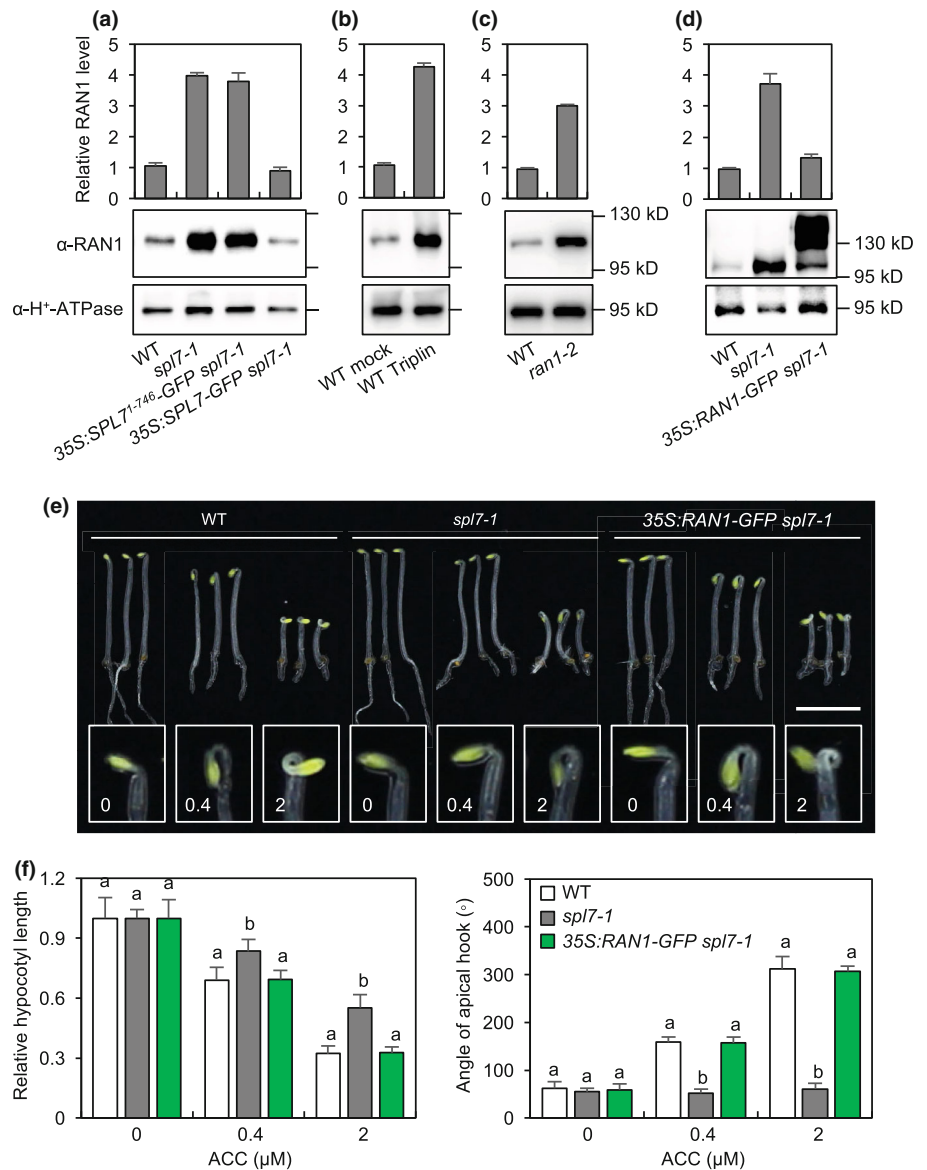
Fig. 7 *SPL7* regulates RAN1 abundance. (a–d) Examination of relative RAN1 abundance in the indicated genotypes using immunoblotting. The wild-type seedlings were also treated with dimethyl sulphoxide (DMSO) (mock) and 10 μM of the copper chelator Triplin. Values are the mean ± SD from three independent experiments. One representative set of blots is shown on the bottom. Size markers are indicated on the right. H⁺-ATPase was used as the loading control. (e) Morphology of etiolated seedlings treated with different concentrations of ACC. Enlarged views show the pical hook of individual seedlings. Bar, 5 mm. (f) Quantification of relative hypocotyl length and angle of the apical hook for the indicated genotypes following 1-amino-cyclopropane-1-carboxylic acid (ACC) treatments. Data represent mean ± SD from 15 individual seedlings. Different letters denote genotypes with significant differences (one-way ANOVA; $P < 0.001$). Experiments were repeated four times with similar results.

(Kropat *et al.*, 2005; Yamasaki *et al.*, 2009; Sommer *et al.*, 2010; Zhang *et al.*, 2014; Yan *et al.*, 2017), it can be postulated that SPL7 may incorporate inputs from Cu homeostasis to dynamically couple ethylene sensitivity to Cu availability in different cell types or over developmental courses. Analysing other components of the Cu delivery and allocation network in relation to ethylene signalling will further elucidate the mechanisms governing regulation and control of the ethylene pathway (Burkhead *et al.*, 2009; Penarrubia *et al.*, 2015). In addition to molecular and modelling efforts, specific probes for monitoring Cu level in different subcellular compartments and tracing intracellular Cu trafficking are highly desired (Hong-Hermesdorf *et al.*, 2014) to improve our understanding of ethylene signalling in the context of plant development and metabolism.

Plant ethylene receptors are derived from the prevalent two-component kinase receptor family in prokaryotes (Chang *et al.*, 1993), presumably via horizontal transfer after endosymbiosis with a cyanobacterium (Mount & Chang, 2002). Consistent with this evolutionary history, ethylene signal transduction is conserved in land plants and green algae (Ju *et al.*, 2015). Phylogenetic analyses revealed that SPL7 is also deeply conserved between green algae and land plants (Kropat *et al.*, 2005; Guo *et al.*, 2008; Sommer *et al.*, 2010). We found that SPL7^TMD is only conserved in angiosperm, but not in green algae and other plant lineages (Fig. S1). This finding together with the fact that the triple response is not in place in the green algae indicates that the TMD of the SPL7 orthologues has specifically evolved in angiosperms to modulate RAN1 function in the context of the triple response. It will be interesting to further elucidate the role of SPL7^TMD, in addition to the triple response, in ethylene-regulated development and adaptation processes that are unique to angiosperm.
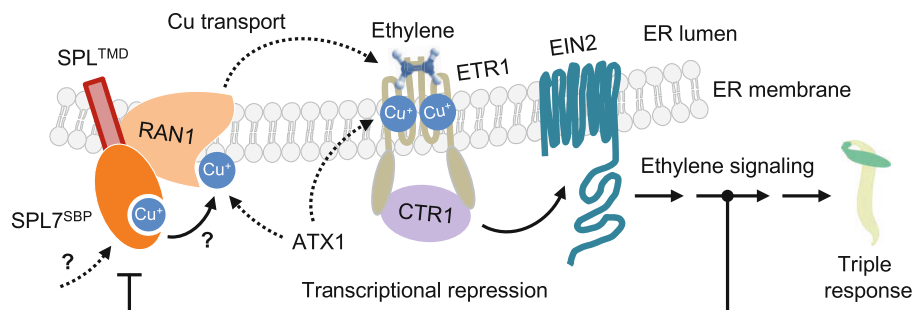
Fig. 8 A model for SPL7 in modulating ethylene sensitivity. ER-located Cu transporter RAN1 is a main component of the ethylene signalling pathway responsible for delivering the monovalent Cu cofactor to the endoplasmic reticulum (ER)-located ethylene receptors represented by ETR1. The Cu-responsive transcription factor SPL7 contains two conserved functional domains: SPL7^{SBP} on the N-terminus that binds Cu and SPL7^{TMD} on the C-terminus that anchors the protein to the ER membrane and interacts with RAN1. The interaction between SPL7 and RAN1 via SPL7^{TMD} is important for regulating ethylene signalling in the triple response either directly by promoting Cu transfer to RAN1 or indirectly by modulating RAN1 abundance. Although the Cu source and the transfer mechanism are not yet known, the SPL7–RAN1 interaction potentially represents an alternative route of the cytosolic Cu transport pathway mediated by the ATX1 family of chaperons. As *SPL7* is transcriptionally repressed by ethylene signalling, indicating by the blunt ended arrow, the SPL7–RAN1 interaction is therefore critical for maintaining proper sensitivity to ethylene. The Cu transport route and ethylene signalling steps are depicted with broken and solid arrows, respectively.

Acknowledgements

Author contributions

LL designed and supervised the research. YY, CH, JD, LX, DL and HC performed the research. YY and ZG analysed the data. HG provided critical materials. YY and LL wrote the paper.

ORCID

Huaqing Cai https://orcid.org/0000-0001-8434-6639
Jianmei Du https://orcid.org/0000-0001-7577-9192
Hongwei Guo https://orcid.org/0000-0003-4819-5874
Zhonglong Guo https://orcid.org/0000-0002-3879-8738
Chen Hao https://orcid.org/0000-0002-7575-3061
Dong Li https://orcid.org/0000-0002-6840-1674
Lei Li https://orcid.org/0000-0001-8304-1286
Lei Xu https://orcid.org/0000-0002-6913-5048
Yanzhi Yang https://orcid.org/0000-0001-5128-7054

Data availability

Sequence data from this article can be found in the Arabidopsis Genome Initiative or GenBank/EMBL databases under the following accession numbers: *RAN1* (At5g44790), *SPL7* (At5g18830), and *EIN3* (At3g20770). T-DNA insertion mutants and other mutants used were: *spl7-1* (SALK_093849C), *ran1-2* (CS3809), *etr1-1* (CS327), and *ctr1-1* (CS8057).

References

Alonso JM, Hirayama T, Roman G, Nourizadeh S, Ecker JR. 1999. EIN2, a bifunctional transducer of ethylene and stress responses in *Arabidopsis. Science* **284**: 2148–2152.

Alonso JM, Stepanova AN, Solano R, Wisman E, Ferrari S, Ausubel FM, Ecker JR. 2003. Five components of the ethylene-response pathway identified in a screen for weak ethylene-insensitive mutants in *Arabidopsis. Proceedings of the National Academy of Sciences, USA* **100**: 2992–2997.

Attar N, Campos OA, Vogelauer M, Cheng C, Xue Y, Schmollinger S, Salwinski L, Mallipeddi NV, Boone BA, Yen L et al. 2020. The histone H3-H4 tetramer is a copper reductase enzyme. *Science* **369**: 59–64.

Banci L, Bertini I, Ciofi-Baffoni S, Kozyreva T, Zovo K, Palumaa P. 2010. Affinity gradients drive copper to cellular destinations. *Nature* **465**: 645–648.

Barghetti A, Sjögren L, Floris M, Paredes EB, Wenkel S, Brodersen P. 2017. Heat-shock protein 40 is the key farnesylation target in meristem size control, abscisic acid signaling, and drought resistance. *Genes & Development* **31**: 2282–2295.

Bernal M, Casero D, Singh V, Wilson GT, Grande A, Yang H, Dodani SC, Pellegrini M, Huijser P, Connolly EL et al. 2012. Transcriptome sequencing identifies SPL7-regulated copper acquisition genes FRO4/FRO5 and the copper dependence of iron homeostasis in *Arabidopsis. Plant Cell* **24**: 738–761.

Berthet S, Demont-Caulet N, Pollet B, Bidzinski P, Cezard L, Le Bris P, Borrega N, Herve J, Blondet E, Balzergue S et al. 2011. Disruption of *LACCASE4* and *17* results in tissue-specific alterations to lignification of *Arabidopsis thaliana* stems. *Plant Cell* **23**: 1124–1137.

Binder BM. 2020. Ethylene signaling in plants. *Journal of Biological Chemistry* **295**: 7710–7725.

Binder BM, Rodriguez FI, Bleecker AB. 2010. The copper transporter RAN1 is essential for biogenesis of ethylene receptors in *Arabidopsis. Journal of Biological Chemistry* **285**: 37263–37270.

Birkenbihl RP, Jach G, Saedler H, Huijser P. 2005. Functional dissection of the plant-specific SBP-domain: overlap of the DNA-binding and nuclear localization domains. *Journal of Molecular Biology* **352**: 585–596.

Burg SP, Burg EA. 1967. Molecular requirements for the biological activity of ethylene. *Plant Physiology* **42**: 144–152.

Burkhead JL, Reynolds KA, Abdel-Ghany SE, Cohu CM, Pilon M. 2009. Copper homeostasis. *New Phytologist* **182**: 799–816.

Chang C, Kwok SF, Bleecker AB, Meyerowitz EM. 1993. Arabidopsis ethylene-response gene *ETR1*: similarity of product to two-component regulators. *Science* **262**: 539–544.

Chang C, Shockey JA. 1999. The ethylene-response pathway: signal perception to gene regulation. *Current Opinion in Plant Biology* **2**: 352–358.

Chang KN, Zhong S, Weirauch MT, Hon G, Pelizzola M, Li H, Huang SS, Schmitz RJ, Urich MA, Kuo D *et al.* 2013. Temporal transcriptional response to ethylene gas drives growth hormone cross-regulation in *Arabidopsis*. *eLife* 2: e00675.

Chao Q, Rothenberg M, Solano R, Roman G, Terzaghi W, Ecker JR. 1997. Activation of the ethylene gas response pathway in *Arabidopsis* by the nuclear protein ETHYLENE-INSENSITIVE3 and related proteins. *Cell* 89: 1133–1144.

Chen YF, Randlett MD, Findell JL, Schaller GE. 2002. Localization of the ethylene receptor ETR1 to the endoplasmic reticulum of *Arabidopsis*. *Journal of Biological Chemistry* 277: 19861–19866.

Cho YH, Yoo SD, Sheen J. 2006. Regulatory functions of nuclear hexokinase1 complex in glucose signaling. *Cell* 127: 579–589.

Clark KL, Larsen PB, Wang X, Chang C. 1998. Association of the *Arabidopsis* CTR1 Raf-like kinase with the ETR1 and ERS ethylene receptors. *Proceedings of the National Academy of Sciences, USA* 95: 5401–5406.

Dubois M, Van den Broeck L, Inze D. 2018. The pivotal role of ethylene in plant growth. *Trends in Plant Science* 23: 311–323.

Finney LA, O'Halloran TV. 2003. Transition metal speciation in the cell: insights from the chemistry of metal ion receptors. *Science* 300: 931–936.

Garcia-Molina A, Xing S, Huijser P. 2014. Functional characterisation of *Arabidopsis* SPL7 conserved protein domains suggests novel regulatory mechanisms in the Cu deficiency response. *BMC Plant Biology* 14: 231.

Guo AY, Zhu QH, Gu X, Ge S, Yang J, Luo J. 2008. Genome-wide identification and evolutionary analysis of the plant specific SBP-box transcription factor family. *Gene* 418: 1–8.

Hirayama T, Alonso JM. 2000. Ethylene captures a metal! Metal ions are involved in ethylene perception and signal transduction. *Plant and Cell Physiology* 41: 548–555.

Hirayama T, Kieber JJ, Hirayama N, Kogan M, Guzman P, Nourizadeh S, Alonso JM, Dailey WP, Dancis A, Ecker JR. 1999. RESPONSIVE-TO-ANTAGONIST1, a Menkes/Wilson disease-related copper transporter, is required for ethylene signaling in *Arabidopsis*. *Cell* 97: 383–393.

Hong-Hermesdorf A, Miethke M, Gallaher SD, Kropat J, Dodani SC, Chan J, Barupala D, Domaille DW, Shirasaki DI, Loo JA *et al.* 2014. Subcellular metal imaging identifies dynamic sites of Cu accumulation in *Chlamydomonas*. *Nature Chemical Biology* 10: 1034–1042.

Hoppen C, Muller L, Hansch S, Uzun B, Milic D, Meyer AJ, Weidtkamp-Peters S, Groth G. 2019. Soluble and membrane-bound protein carrier mediate direct copper transport to the ethylene receptor family. *Scientific Reports* 9: 10715.

Ishka MR, Chia JC, Vatamaniu OK. 2022. Advances in understanding of copper function and transport in plants. In: Upadhyay SK, ed. *Cation transporters in plants*. Cambridge, MA, USA: Academic Press, 205–226.

Jiang A, Guo Z, Pan J, Yang Y, Zhuang Y, Zuo D, Hao C, Gao Z, Xin P, Chu J *et al.* 2021. The PIF1-miR408-PLANTACYANIN repression cascade regulates light-dependent seed germination. *Plant Cell* 33: 1506–1529.

Jing Y, Sun H, Yuan W, Wang Y, Li Q, Liu Y, Li Y, Qian W. 2016. SUVH2 and SUVH9 couple two essential steps for transcriptional gene silencing in *Arabidopsis*. *Molecular Plant* 9: 1156–1167.

Johnson PR, Ecker JR. 1998. The ethylene gas signal transduction pathway: a molecular perspective. *Annual Review of Genetics* 32: 227–254.

Ju C, Van de Poel B, Cooper ED, Thierer JH, Gibbons TR, Delwiche CF, Chang C. 2015. Conservation of ethylene as a plant hormone over 450 million years of evolution. *Nature Plants* 1: 14004.

Katoh S. 1960. A new copper protein from *Chlorella ellisoidea*. *Nature* 186: 533–534.

Kieber JJ, Rothenberg M, Roman G, Feldmann KA, Ecker JR. 1993. CTR1, a negative regulator of the ethylene response pathway in *Arabidopsis*, encodes a member of the raf family of protein kinases. *Cell* 72: 427–441.

Kropat J, Tottey S, Birkenbihl RP, Depege N, Huijser P, Merchant S. 2005. A regulator of nutritional copper signaling in *Chlamydomonas* is an SBP domain protein that recognizes the GTAC core of copper response element. *Proceedings of the National Academy of Sciences, USA* 102: 18730–18735.

Kumar S, Stecher G, Li M, Knyaz C, Tamura K. 2018. MEGA X: molecular evolutionary genetics analysis across computing platforms. *Molecular Biology and Evolution* 35: 1547–1549.

Langmead B, Salzberg SL. 2012. Fast gapped-read alignment with Bowtie 2. *Nature Methods* 9: 357–359.

Li W, Lacey RF, Ye Y, Lu J, Yeh KC, Xiao Y, Li L, Wen CK, Binder BM, Zhao Y. 2017. Triplin, a small molecule, reveals copper ion transport in ethylene signaling from ATX1 to RAN1. *PLoS Genetics* 13: e1006703.

Li W, Ma M, Feng Y, Li H, Wang Y, Ma Y, Li M, An F, Guo H. 2015. EIN2-directed translational regulation of ethylene signaling in *Arabidopsis*. *Cell* 163: 670–683.

Liu Q, Wang F, Axtell MJ. 2014. Analysis of complementarity requirements for plant microRNA targeting using a *Nicotiana benthamiana* quantitative transient assay. *Plant Cell* 26: 741–753.

Merchant SS, Schmollinger S, Strenkert D, Moseley JL, Blaby-Haas CE. 2020. From economy to luxury: copper homeostasis in *Chlamydomonas* and other algae. *Biochimica et Biophysica Acta – Molecular Cell Research* 1867: 118822.

Merchante C, Alonso JM, Stepanova AN. 2013. Ethylene signaling: simple ligand, complex regulation. *Current Opinion in Plant Biology* 16: 554–560.

Mount SM, Chang C. 2002. Evidence for a plastid origin of plant ethylene receptor genes. *Plant Physiology* 130: 10–14.

Nelson BK, Cai X, Nebenfuhr A. 2007. A multicolored set of *in vivo* organelle markers for co-localization studies in *Arabidopsis* and other plants. *The Plant Journal* 51: 1126–1136.

Penarrubia L, Romero P, Carrio-Segui A, Andres-Borderia A, Moreno J, Sanz A. 2015. Temporal aspects of copper homeostasis and its crosstalk with hormones. *Frontiers in Plant Science* 6: 255.

Qiao H, Shen Z, Huang SS, Schmitz RJ, Urich MA, Briggs SP, Ecker JR. 2012. Processing and subcellular trafficking of ER-tethered EIN2 control response to ethylene gas. *Science* 338: 390–393.

Rae TD, Schmidt PJ, Pufahl RA, Culotta VC, O'Halloran TV. 1999. Undetectable intracellular free copper: the requirement of a copper chaperone for superoxide dismutase. *Science* 284: 805–808.

Robinson NJ, Winge DR. 2010. Copper metallochaperones. *Annual Review of Biochemistry* 79: 537–562.

Rodriguez FI, Esch JJ, Hall AE, Binder BM, Schaller GE, Bleecker AB. 1999. A copper cofactor for the ethylene receptor ETR1 from *Arabidopsis*. *Science* 283: 996–998.

Solano R, Stepanova A, Chao Q, Ecker JR. 1998. Nuclear events in ethylene signaling: a transcriptional cascade mediated by ETHYLENE-INSENSITIVE3 and ETHYLENE-RESPONSE-FACTOR1. *Genes & Development* 12: 3703–3714.

Sommer F, Kropat J, Malasarn D, Grossoehme NE, Chen X, Giedroc DP, Merchant SS. 2010. The CRR1 nutritional copper sensor in *Chlamydomonas* contains two distinct metal-responsive domains. *Plant Cell* 22: 4098–4113.

Weigel M, Varotto C, Pesaresi P, Finazzi G, Rappaport F, Salamini F, Leister D. 2003. Plastocyanin is indispensable for photosynthetic electron flow in *Arabidopsis thaliana*. *Journal of Biological Chemistry* 278: 31286–31289.

Wen X, Zhang C, Ji Y, Zhao Q, He W, An F, Jiang L, Guo H. 2012. Activation of ethylene signaling is mediated by nuclear translocation of the cleaved EIN2 carboxyl terminus. *Cell Research* 22: 1613–1616.

Woeste KE, Kieber JJ. 2000. A strong loss-of-function mutation in *RAN1* results in constitutive activation of the ethylene response pathway as well as a rosette-lethal phenotype. *Plant Cell* 12: 443–455.

Xie Y, Liu Y, Wang H, Ma X, Wang B, Wu G, Wang H. 2017. Phytochrome-interacting factors directly suppress *MIR156* expression to enhance shade-avoidance syndrome in Arabidopsis. *Nature Communications* 8: 348.

Yamasaki H, Hayashi M, Fukazawa M, Kobayashi Y, Shikanai T. 2009. SQUAMOSA promoter binding protein-like7 is a central regulator for copper homeostasis in *Arabidopsis*. *Plant Cell* 21: 347–361.

Yamasaki K, Kigawa T, Inoue M, Tateno M, Yamasaki T, Yabuki T, Aoki M, Seki E, Matsuda T, Nunokawa E *et al.* 2004. A novel zinc-binding motif revealed by solution structures of DNA-binding domains of *Arabidopsis* SBP-family transcription factors. *Journal of Molecular Biology* 337: 49–63.

Yan J, Chia JC, Sheng H, Jung HI, Zavodna TO, Zhang L, Huang R, Jiao C, Craft EJ, Fei Z *et al.* 2017. Arabidopsis pollen fertility requires the transcription factors CITF1 and SPL7 that regulate copper delivery to anthers and jasmonic acid synthesis. *Plant Cell* 29: 3012–3029.

Yang Y, Li D, Chao X, Singh SP, Thomason P, Yan Y, Dong M, Li L, Insall RH, Cai H. 2021. Leep1 interacts with PIP3 and the Scar/WAVE complex to

regulate cell migration and macropinocytosis. *Journal of Cell Biology* 220: e202010096.

Yang Z, Wang X, Gu S, Hu Z, Xu H, Xu C. 2008. Comparative study of SBP-box gene family in *Arabidopsis* and rice. *Gene* 407: 1–11.

Yatsunyk LA, Rosenzweig AC. 2007. Cu(I) binding and transfer by the N terminus of the Wilson disease protein. *Journal of Biological Chemistry* 282: 8622–8631.

Zhang H, Li L. 2013. SQUAMOSA promoter binding protein-like7 regulated microRNA408 is required for vegetative development in *Arabidopsis. The Plant Journal* 74: 98–109.

Zhang H, Zhao X, Li J, Cai H, Deng XW, Li L. 2014. MicroRNA408 is critical for the HY5-SPL7 gene network that mediates the coordinated response to light and copper. *Plant Cell* 26: 4933–4953.

Zhao XC, Qu X, Mathews DE, Schaller GE. 2002. Effect of ethylene pathway mutations upon expression of the ethylene receptor ETR1 from *Arabidopsis. Plant Physiology* 130: 1983–1991.

Zhuang Y, Zuo D, Tao Y, Cai H, Li L. 2020. Laccase3-based extracellular domain provides possible positional information for directing Casparian strip formation in *Arabidopsis. Proceedings of the National Academy of Sciences, USA* 117: 15400–15402.

Supporting Information

Additional Supporting Information may be found online in the Supporting Information section at the end of the article.

Fig. S1 Angiosperm SPL7 orthologues contain a C-terminal transmembrane domain.

Fig. S2 Schematic depiction of SPL7 domains and various truncated forms for subcellular localisation analysis.

Fig. S3 Absence of the TMD results in exclusive nuclear localisation of SPL7.

Fig. S4 Subcellular localisation of the N-terminal and C-terminal portions of SPL7 expressed in Arabidopsis.

Fig. S5 Confirmation of RAN1 interaction with SPL7 using yeast-two-hybrid assay.

Fig. S6 Verification of the RAN1 antibody.

Fig. S7 Co-IP analysis of the interaction between full-length SPL7 and RAN1 in Arabidopsis.

Fig. S8 Verification of RAN1 localisation on the ER.

Fig. S9 Characterisation of *SPL7*-related transgenic lines.

Fig. S10 Phenotypic analysis of *SPL7*-related transgenic lines.

Fig. S11 The TMD of SPL7 is required for ethylene response.

Fig. S12 Ethylene signalling mutants are insensitive to Triplin.

Fig. S13 The *spl7-1* mutant is hypersensitive to the Cu chelator BCS.

Fig. S14 Cu content in whole seedlings.

Fig. S15 Examination of *RAN1* transcript levels.

Fig. S16 Feedback regulation of *SPL7* transcription using ethylene signalling.

Table S1 Oligonucleotide sequences of the primers used in this study.

Table S2 RT-qPCR data from three independent experiments whereby data from Expt. 1 were used for generating the figures.

Table S3 Accession numbers of SPL7 orthologues.

Table S4 Putative SPL7^{TMD}-interacting proteins identified using IP-MS/MS.

Please note: Wiley Blackwell are not responsible for the content or functionality of any Supporting Information supplied by the authors. Any queries (other than missing material) should be directed to the *New Phytologist* Central Office.